



University of HUDDERSFIELD

University of Huddersfield Repository

Trevor, Susannah L, Butler, Michael F., Adams, Sarah, Laity, Peter R., Burley, Jonathan C. and Cameron, Ruth E.

Structure and phase transitions of genipin, an herbal medicine and naturally occurring cross-linker

Original Citation

Trevor, Susannah L, Butler, Michael F., Adams, Sarah, Laity, Peter R., Burley, Jonathan C. and Cameron, Ruth E. (2008) Structure and phase transitions of genipin, an herbal medicine and naturally occurring cross-linker. *Crystal Growth and Design*, 8 (5). pp. 1748-1753. ISSN 1528-7483

This version is available at <http://eprints.hud.ac.uk/13424/>

The University Repository is a digital collection of the research output of the University, available on Open Access. Copyright and Moral Rights for the items on this site are retained by the individual author and/or other copyright owners. Users may access full items free of charge; copies of full text items generally can be reproduced, displayed or performed and given to third parties in any format or medium for personal research or study, educational or not-for-profit purposes without prior permission or charge, provided:

- The authors, title and full bibliographic details is credited in any copy;
- A hyperlink and/or URL is included for the original metadata page; and
- The content is not changed in any way.

For more information, including our policy and submission procedure, please contact the Repository Team at: E.mailbox@hud.ac.uk.

<http://eprints.hud.ac.uk/>

Structure and Phase Transitions of Genipin, An Herbal Medicine and Naturally Occurring Cross-Linker

Susannah L. Trevor,^{*,†} Micheal F. Butler,[‡] Sarah Adams,[‡] Peter R. Laity,[†]
Jonathan C. Burley,[§] and Ruth E. Cameron[†]

University of Cambridge, Department of Materials Science and Metallurgy, Pembroke Street,
Cambridge, CB2 3QZ, U.K., Unilever R&D Colworth, Sharnbrook, Bedford, MK44 1LQ, U.K., and
University of Cambridge, Department of Chemistry, Lensfield Road, Cambridge, CB2 1EW, U.K.

Received June 20, 2007; Revised Manuscript Received January 14, 2008

ABSTRACT: The naturally occurring cross-linking agent genipin has recently been the subject of biomedical research both in the creation of hydrogel structures and as a potential active agent in its own right. In this study several methods of specimen preparation were used to isolate and stabilize crystalline genipin material. The thermodynamic properties of the genipin crystals and their phase changes were investigated using differential scanning calorimetry techniques. Single crystal and powder X-ray diffraction (XRD) confirmed two separate polymorphic phases denoted form I and form II. The structures were resolved, and the XRD traces were indexed, and both forms were found to be monoclinic. Genipin forms I and II were also isolated through methanol evaporation crystallization. Form II was formed through this route when the crystallization was accompanied by polymerization of a fraction of the genipin. The materials were also tested under in situ heated, X-ray diffraction conditions at a synchrotron radiation source. Genipin forms I and II were shown to have melting temperatures of around 121 and 101 °C, respectively.

Introduction

The naturally occurring cross-linking agent genipin (Figure 1) has recently been the subject of biomedical research both in the creation of hydrogel structures and as a potential active agent on its own as a potential treatment for type II diabetes.^{1–3} Because of the numerous and wide ranging fields of genipin research currently being carried out, it is increasingly pertinent to consider the nature of the substrate itself. Understanding the variations in the crystal packing of a molecule, otherwise known as polymorphism, is essential as it determines a host of the material's structural properties. This is particularly crucial in the pharmaceutical industry where the solid state behavior may determine the dissolution rate, equilibrium solubility, and absorption rate or even if the agent is wholly unsuitable for therapy.⁴ Additionally, prior knowledge of any polymorphic behavior is important if the agent is going to be presented for regulatory approval. In this study, preliminary tests on the thermodynamic behavior of genipin revealed multiple melting events indicating some interesting crystalline behavior, and it is the ambition of this study to further investigate the crystallographic nature of this small molecule. The effects of genipin polymerization on crystallinity are also investigated. This was done using a combination of optical microscopy, differential scanning calorimetry (DSC), and X-ray diffraction (XRD) techniques.

Experimental Procedures

Materials Preparation. Genipin was obtained from Challenge Bioproducts Co. Ltd. Taiwan, was used in the as-supplied state, and also was prepared in several other states.

Form I Crystal Preparation. Slow evaporation from a 50 mM genipin/methanol solution at room temperature led to the formation of small crystals suitable for analysis by single crystal diffraction methods. These crystals were later denoted form I.

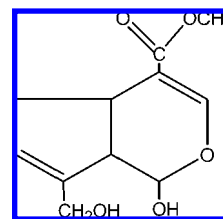


Figure 1. The chemical structure of genipin.

Form II Crystal Isolation. As we were unable to grow single crystals suitable for structure determination from single-crystal diffraction, form II genipin was prepared in a 0.7 mm Lindemann glass capillary inside a Mettler Toledo DSC822e. The sample was then heated under nitrogen to 130 °C to form a melt and quenched to room temperature. This produced crystals that were later denoted form II.

Genipin Crystallized by Slow Methanol Evaporation. A supersaturated solution of roughly 120 mM genipin in laboratory grade methanol was prepared and covered to allow a slow evaporation. As evaporation occurred, the genipin solution crystallized. It was found that in some samples polymerization occurred and that within the polymerized genipin pockets of crystals would grow. These crystals were removed for analysis. In other samples where the polymerization reaction did not occur, the entire sample was crystalline after evaporation, and these crystals were also analyzed.

Optical Microscopy. A sapphire crucible containing as supplied genipin was placed on a glass coverslip and heated on a hot stage under the microscope. Crossed polars were used. A heating, cooling, reheating cycle was performed. An initial 25 °C temperature was raised to 130 °C and equilibrated for 2 min before cooling again to 25 °C. A further 2 min equilibration was applied and another reheat was conducted again to 130 °C. A constant heating/cooling rate of 6 °C min⁻¹ was used throughout.

DSC. Differential scanning calorimetry was carried out using a TA Instruments Q1000 DSC, which uses the heat flux method. Samples of mass between 20 and 40 mg were accurately weighed into aluminum pans. A heating rate of 6 or 10 °C min⁻¹ was used to heat the sample from -25 to 130 °C. Samples were then quenched to -25 °C at a cooling rate of between 50 and 100 °C min⁻¹.

XRD. Single Crystal XRD and Structure Resolution. The single crystal X-ray diffraction was carried out at -93 °C on Nonius CCD diffractometer using molybdenum K α 1 radiation (0.71 Å). The data were recorded over a 2-theta range of 3.85–27.49°. The cell refinement

* To whom correspondence should be addressed: Susie Trevor, Sintef Materialer og Kjemi, P.O. Box 124, Blindern, 0314, Oslo, Norway. E-mail: st328@cam.ac.uk.

[†] University of Cambridge, Department of Materials Science and Metallurgy.

[‡] Unilever R&D Colworth.

[§] University of Cambridge, Department of Chemistry.

was standard data reduction using HKL methods⁵ and structure solving and refinement was carried out using SHELXL9.⁶

XRD of Form II and Structure Resolution. Powder X-ray diffraction traces of form II genipin formed in the Lindemann capillary were made at room temperature using a stoe Stadi-P diffractometer, operating in Dybye-Scherrer geometry, using Cobalt $K\alpha_1$ radiation (1.78 Å). The data were recorded over a 2-theta range of 2–80° with a step size of 0.01 and a time of 2 s per step. We were able to successfully index the pattern, solve the structure through the standard methods, which was refined, and the proposed structural model yielded an excellent agreement with the calculated pattern and a chemically reasonable structural model.

Powder X-ray Diffraction. PXRD was carried out on the “as-supplied” genipin, and the crystals formed by methanol evaporation. Wide angle X-ray scattering (WAXS) experiments were conducted at room temperature using a Phillips diffractometer, with Copper $K\alpha_1$ radiation (1.54 Å). The data were recorded over a 2-theta range of 5–50°, with a step size of 0.05 and a time of 2 s per step.

In Situ Powder X-ray Diffraction. Further wide-angle X-ray scattering was carried out station 6.2 of the Darresbury Synchrotron radiation source, Cheshire, UK. The samples were enclosed in aluminum pans and heated using a heating stage at a rate of 10 °C/min from 25 to 130 °C to correspond with the DSC experiments. The detector type is a medium-high resolution curved 1-dimensional WAXS detector. Diffraction data were binned at 6 s intervals. The data were background subtracted and normalized.

Molecular Graphics. Once the structures of each form were resolved, the Mercury software version 1.4.1 from the Cambridge Crystallographic Data Centre (CCDC) was used for creating the molecular graphics.

Results

DSC. Figure 2a shows the DSC trace of the genipin in the “as-supplied” state (form I). The material is crystalline, and a single melting transition is seen at 121 °C ($\Delta H_m = 32.3$ kJ/mol). A second heating cycle was carried out on the genipin melt after a fast quenched cooling (Figure 2b). At a heating rate of 10 °C min⁻¹, the onset of crystallization is observed between 55 and 87 °C ($\Delta H_m = 2.6$ kJ/mol), an initial melting peak is seen at 97.4 °C, and a final melting peak is seen at 101.4 °C (total $\Delta H_m = 3.6$ kJ/mol). Heating at 6 °C min⁻¹ (to match the optical microscope experiment) (Figure 3) resulted in slightly better separated peaks, but little significant difference in behavior. Figure 2c shows the DSC trace of crystals prepared by the methanol evaporation method and extracted from a sample in which polymerization did not occur. In this case a crystallization can be seen between 98 and 105 °C followed by a broad melting peak at 119 °C.

Figure 2d shows the DSC trace of crystals extracted from a sample in which polymerization did occur. The DSC data shows a very broad melting peak from around 90–110 °C ($\Delta H_m = 1.60$ kJ/mol), which implies a lesser degree of crystallinity in this sample. The T_m occurs at approximately 105 °C. A second smaller melting peak is also observable at 115 °C.

Optical Microscopy. Figure 3 shows the images obtained during the optical microscopy observations during heating/cooling/reheating of as-supplied genipin. Initially, block-like crystals are observable, and no visible changes take place during heating until around 121 °C, but by 127 °C all crystals have completely melted. During the cooling part of the cycle, there are no observable effects until the temperature is lowered to 50 °C when small needle-like crystals appear. Only a small amount of crystal growth occurs during the rest of the cooling cycle. However, once the reheating cycle begins, the seeded crystals propagate significantly, showing a needle-like crystal form. Despite the greater crystal growth during this phase, there are still some patches of the amorphous melt phase visible. At just under 100 °C, a second crystal system forms. This second crystal

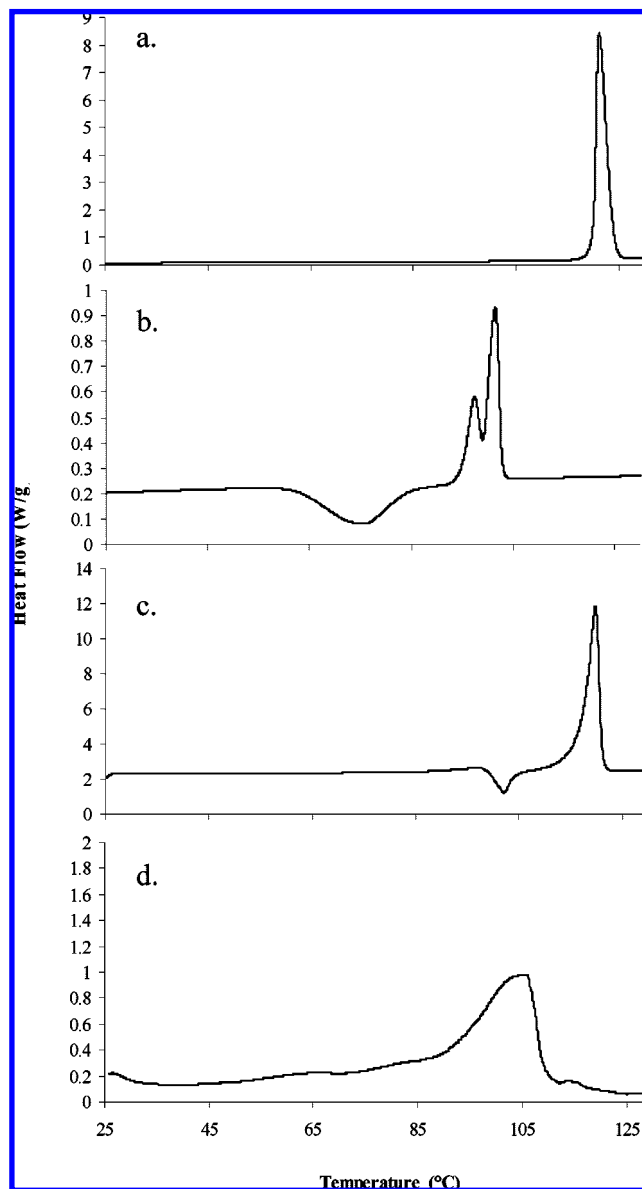


Figure 2. DSC data from 10 °C min⁻¹ heating of (a) form I genipin, (b) reheating of the fast quenched genipin melt, (c) genipin crystals prepared by methanol evaporation methods where no polymerization reaction occurred, (d) genipin crystals formed by methanol evaporation where polymerization did occur.

growth appears to have initiated out of the field of view so was likely to have actually begun growth at a temperature lower than 100 °C. The second crystal growth continues, but it is unclear whether it is formed by the transformation of the first crystal type or is forming concurrently from the melt. This continues until around 103 °C when there is an apparent melting of the original phase leaving the second phase only, which continues to grow until a complete melting at around 121 °C.

X-Ray Diffraction. Single crystal XRD was carried out, the structural model was developed, and a Rietveld refinement carried out. It was found to have a monoclinic B unit cell (b-unique); $a=7.53360$, $b=17.68770$, $c=8.14160$ Å, and $\beta 94.877^\circ$. Figure 3a shows the refined and indexed model from the single crystal data (the broken line). This has been denoted form I.

The as-supplied genipin was in the form of a crystalline powder. When PXRD was carried out the as-supplied genipin was found to have the form I structure, and this is demonstrated

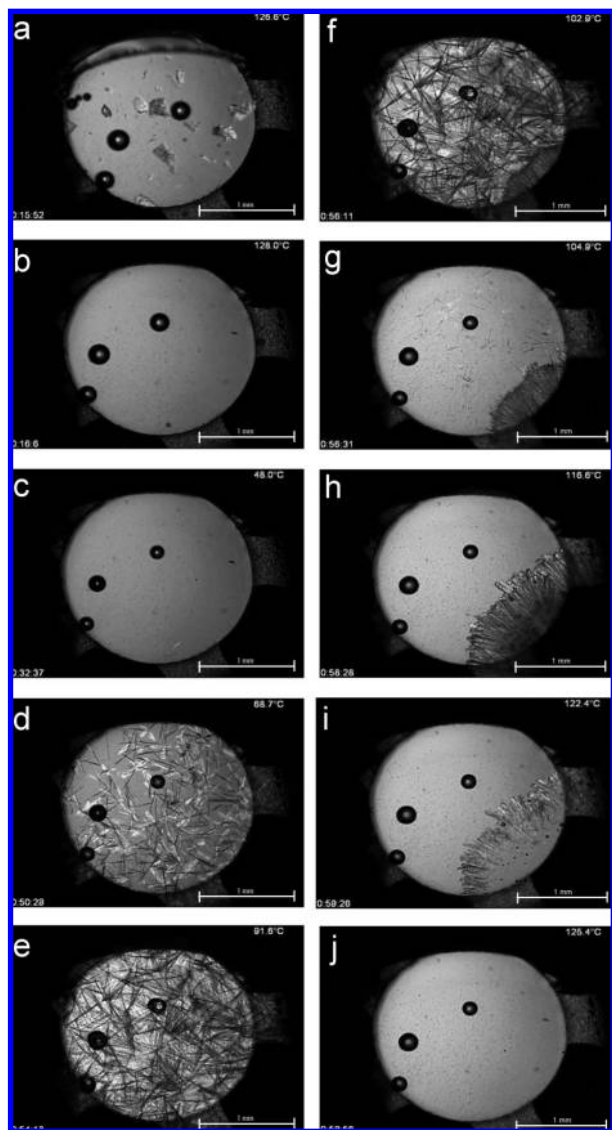


Figure 3. (a–j) Optical microscopy images collected during a heating/cooling/reheating cycle. From 25 to 130 °C, cooled to 25 °C and reheated to 130 °C at a rate of 6 °C min⁻¹.

where is shown overlaying the Rietveld refinement in Figure 4A. The inconsistency between the two plots are due to temperature differences in the experimental setup. The single crystal XRD was carried out at -90 °C, and the Rietveld refinement is derived from this data. The PXRD on the as-supplied genipin was carried out at room temperature. The effect of increasing temperature on the crystal structure is demonstrated by the in situ XRD.

The same heating conditions as used in the DSC experiments (10 °C min⁻¹) were repeated using synchrotron radiation to collect time-resolved XRD patterns of the sample during the scan (Figure 4B). The data was relatively low resolution but did reveal changes in the form I crystals on heating, specifically the merging of the (11 $\bar{1}$) and (111), the (12 $\bar{1}$) and the (121), and the (13 $\bar{1}$) and the (131) reflections, above 100 °C. This was attributed to thermal expansion.

A second, less stable polymorph of genipin as evidenced in the second heating cycle in the DSC was not possible to isolate as a single crystal but a powder form was tested. The powder XRD diffraction pattern and indices are shown in Figure 5A. The resolved structure was found to be monoclinic C2; *a*-20.8243,

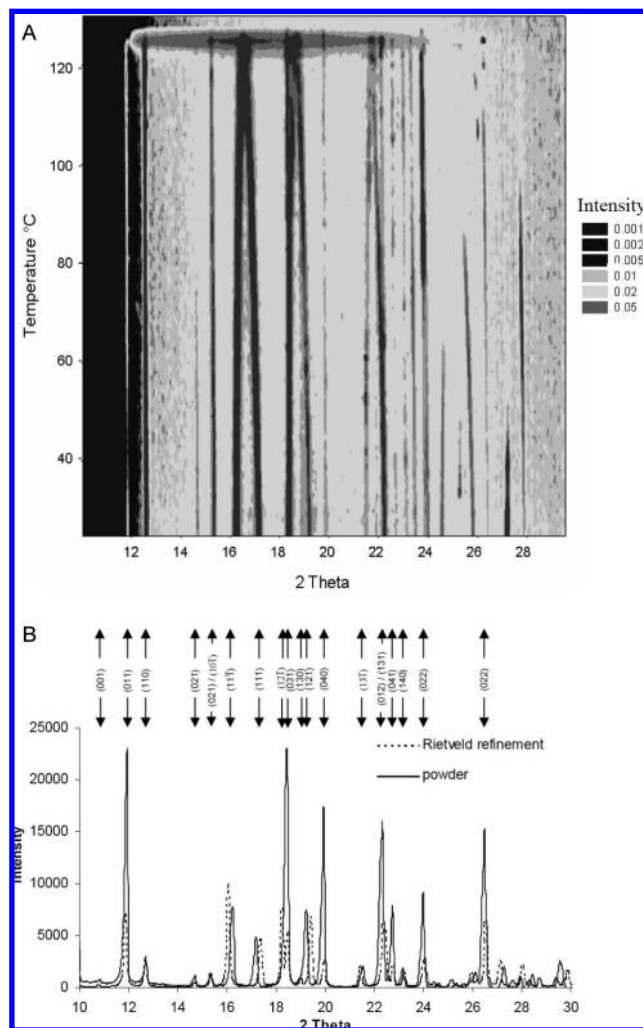


Figure 4. (A) 3D heating in situ powder XRD trace of form I genipin (data obtained using a wavelength of 1.54 Å) and (B) refined structure of form I genipin modelled from the single crystal XRD and PXRD pattern of form I genipin (data obtained using a wavelength of 1.54 Å).

b-6.06204, *c*-8.5848 Å, and β -90.526° (goodness of fit; $\chi^2 = 1.341$ for 107 variables, $R_p = 0.00466$, $R_{wp} = 0.0364$). We have denoted this structure form II of genipin.

A reheating cycle was performed on the as-supplied genipin during the in situ XRD. The resulting diffraction pattern was found to match that of form I, although the data sets in Figure 4A,B were obtained at different wavelengths and as such are represented offset from each other. Investigations using the Mercury crystallographic software showed the Rietveld refined structure matched that obtained in situ when adjusted for the lower wavelength. This in situ heating XRD performed on the quenched melt shows the beginnings of crystal formation around 50 °C and T_m at 105 °C (Figure 5B). No peak merging is observed in this sample.

Powder XRD carried out on the genipin crystallized by methanol evaporation where polymerization did not occur shows a similar diffraction pattern to that of the form I genipin (Figure 6A). During the in situ XRD studies, this material shows the XRD pattern of form I at the lower temperatures (Figure 6B). The same peak merging pattern as observed in the as-received is also observable, although this is onset at a slightly lower 90 °C and melting is observed at around 118 °C.

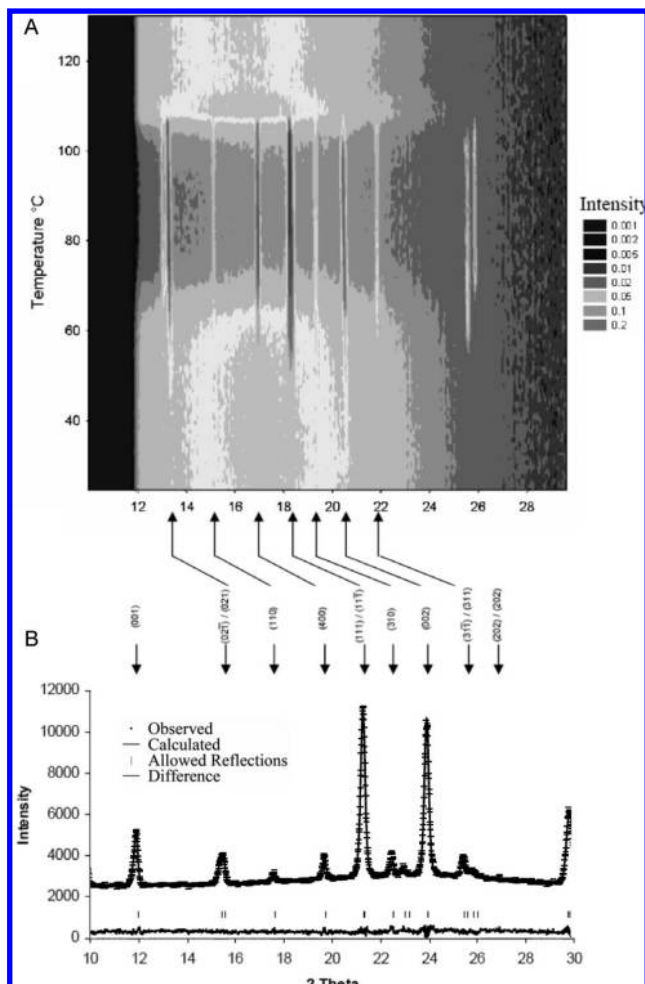


Figure 5. (A) 3D heating in situ XRD traces for form II genipin formed in situ from the quenched melt, undergoing heating from 25 to 130 °C (data obtained using a wavelength of 1.54 Å) and (B) refined structure of form II genipin modelled from PXRD and PXRD pattern of form II genipin (data obtained using a wavelength of 1.78 Å).

The crystals obtained from the sample in which polymerization occurred shows a diffraction pattern consistent with that of form II genipin (Figure 6C), as it has the (201) and 002 peaks, but there was also some distinction between the refractive equivalent planes such as (11 $\bar{1}$) and (111) as was observed in the form I samples. The in situ data exhibits the same form II diffraction pattern until approximately 97 °C upon which point the (201) and (002) diffraction planes indicative of form II genipin disappear leaving the pattern typical of form I genipin, including the peak merging behavior (Figure 6D).

Molecular Graphics. Three-dimensional models of the resolved unit cells were created based on the models of form I and II genipin using Mercury crystallographic software. These are shown in Figure 7.

Discussion

The Polymorphic Structures of Genipin. In the experiments performed, there is evidence of the formation of two different crystal structures: one more stable form, denoted form I, and a second less stable form, form II. Samples of each form were isolated, and using single crystal and powder XRD the two structures were refined and the structures resolved. Figures 4A and 5A (the broken line patterns) show the indexed diffraction

patterns of the two forms. Notable differences are the presence of the (201) and (002) peaks which appear only in the form II structure.

By looking at models in Figure 7a,b of the two forms, it is possible to see conformational polymorphism between the two structures. Rotation of the -CH₂OH group accounts for the different packing and unit cells shown in Figure 6C,D. In the case of form I, the packing leads to a three-dimensional network of hydrogen bonding. However, in form II the hydrogen bonding occurs in horizontal layers only. The more integral bonding in form I helps to explain the increased stability and higher T_m . The planar packing type in form II would also affect the solubility, mechanical strength, and compressibility, which may have implications for product manufacture.

As Supplied Genipin (Form I). Using optical microscopy, the as-supplied genipin exhibited a simple melting reaction at approximately 126 °C, as shown in Figure 3. This behavior was repeated when as-supplied genipin was heated in DSC. Figure 2a shows a single melting event at 121 °C suggesting that the as-supplied genipin is a single crystal phase that does not undergo and transformations while heated in this range.

Examination of the structure using PXRD, as shown in Figure 4A the solid line, revealed that as-supplied genipin had the form I structure. The in situ XRD experiments allowed us to track any phase changes that may be occurring during heating. The as-supplied genipin sample was confirmed again to have the form I structure at room temperature.

Quenched and Reheated Genipin (Form II). During the reheating cycle of the optical microscopy, there seemed to be the formation of two separate phases. The first crystal growth phase from the crystal melt was observable during reheating from the melt at about 70 °C. This phase begins to disappear when the next phase grows at around 100 °C. It is unclear whether this second crystal phase is forming from the melt or the original phase is transforming. The second crystal phase melts at around 120 °C. The lower melting temperature and possible transformation suggest the lesser stability form (form II) was the first observable crystal phase. The other crystals, probably form I, was more stable and thus melted at a higher temperature.

When the quenched genipin was inspected with DSC (Figure 2b), crystallization was observed at around 70 °C as for the optical microscopy, followed by a double melting endotherm at 97 and 101 °C. This double melting is indicative of either the melting of two different forms or the melting event of a single form (form II) with a concurrent crystal perfection event occurring in the middle of it.

The optical microscopy observations (Figure 3) were performed, while the as-supplied genipin was being heated, cooled, and reheated under similar heating/cooling conditions as those used for the DSC experiments (which were repeated at the slightly slower rate of 6 °C min⁻¹ and were the same as with the 10 °C heating rate shown in Figure 2), and one would expect the results to be comparable. However, the complete melting of the DSC samples by 101 °C is in direct contrast to the melting of the second phase of crystals in the optical microscope at around 120 °C. This inconsistency is probably due to differing nucleation conditions, one experiment being carried out in an aluminum DSC pan, the other on a glass microscope slide. It seems probable that the crystallization of form I crystals in the optical microscope did not occur in the DSC.

The in situ XRD observation of the genipin quenched from the melt (Figure 5B) was performed on samples held in aluminum pans as for the DSC experiments. The results

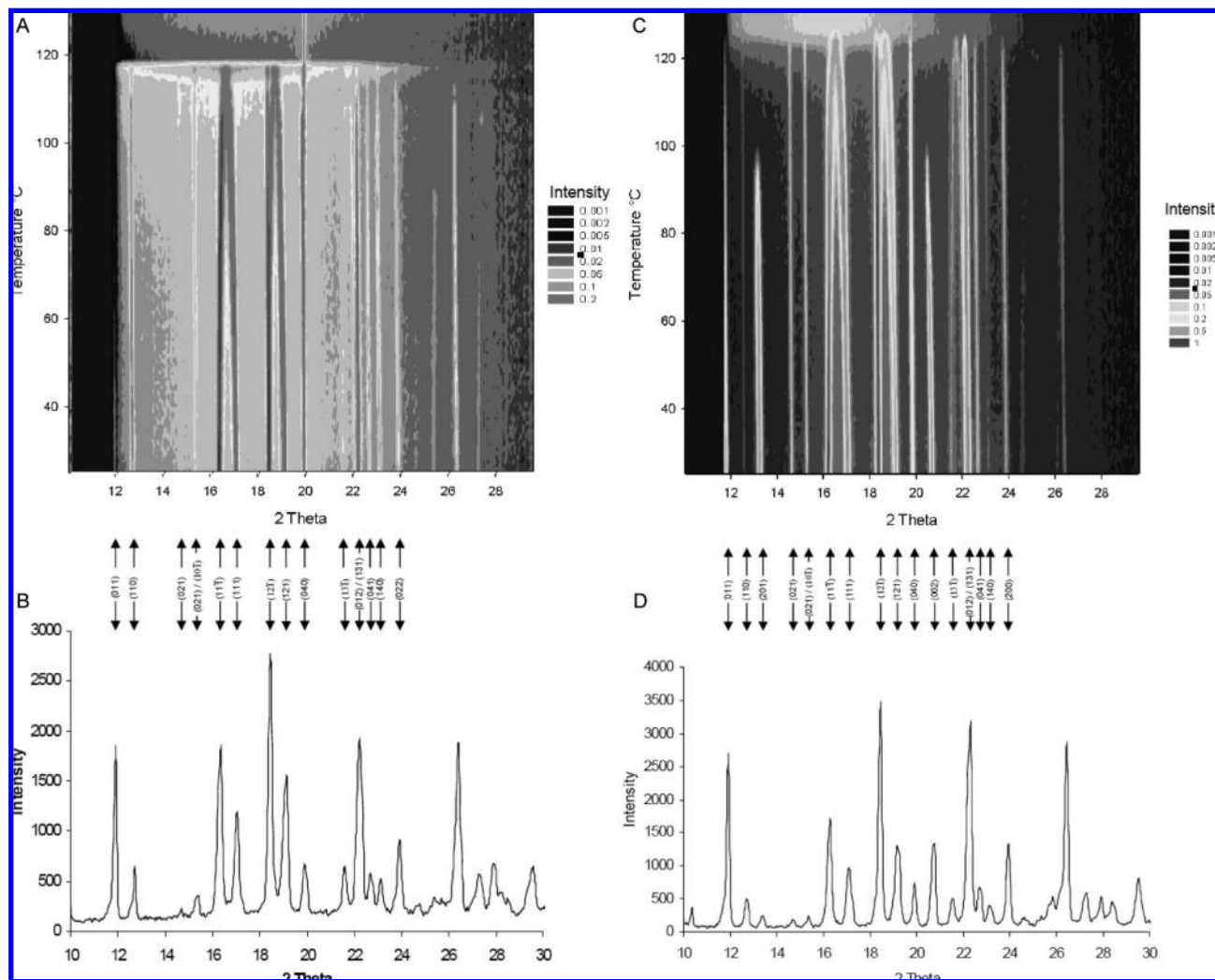


Figure 6. (A) heating in situ XRD data of genipin crystallized by methanol evaporation where no polymerization reaction occurred (data obtained using a wavelength of 1.54 Å), (B) PXRD trace of genipin crystallized by methanol evaporation where no polymerization reaction occurred (data obtained using a wavelength of 1.54 Å), (C) heating in situ XRD data of genipin crystallized by methanol evaporation where a polymerization reaction occurred (data obtained using a wavelength of 1.54 Å), (D) PXRD trace of genipin crystallized by methanol evaporation where a polymerization reaction occurred (data obtained using a wavelength of 1.54 Å).

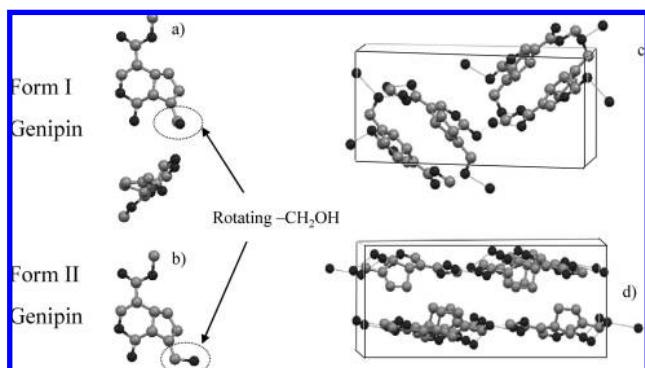


Figure 7. Resolved unit cell of form I genipin (a) form II (b) and the three-dimensional models showing the molecular packing of (c) form I and (d) form II.

confirmed the crystallization of form II genipin, as evidenced again by the presence of the form II specific (201) and (002) diffraction planes. This quenched sample shows only amorphous material as the sample is heated, until crystal formation begins between 50 and 70 °C. During heating there is no evidence of

any phase change occurring. This suggests that the double melting event observed under the same heating and nucleation conditions in the DSC experiments is not a phase change but rather due to a crystal perfection event. Melting occurs at 105 °C, and no further crystal phase is observable.

Crystallization from Methanol Evaporation and the Effect of Partial Genipin Polymerization. It was found that the presence of polymerized genipin affected the crystal growth of the remaining (presumably monomer) genipin.

The XRD observations of the crystalline material extracted from methanol evaporation where no polymerization occurred show the genipin had a form I structure (Figure 6A). However its thermal properties were slightly altered from that of the as-supplied form I genipin. The DSC trace (Figure 2c) showed some crystallization occurred and melting occurred at 119 °C, slightly lower than observed previously for a form I crystal type. The in situ XRD data (Figure 6B) showed a spectrum consistent with the form I structure but also had a lower melting point, around 118 °C. The spectra show a larger amount of peak broadening than those of the as-supplied form I genipin. This suggests a greater degree of crystal imperfec-

tion, which explains the depressed T_m . The similarities between the supplied form I genipin and the form I genipin from methanol evaporation are also demonstrated in the in situ XRD data (Figure 6B). In this case, it is possible again to observe the $(11\bar{1})$ and (111) , $(12\bar{1})$ and (121) , $(13\bar{1})$ and (131) peaks converging as the temperature rises.

XRD data at room temperature (Figure 6C) show form I and form II genipin are present in the material crystallized in the methanol evaporation sample where polymerization did occur. The DSC curve (Figure 2d) shows a very broad melting transition from 90 to 110 °C. In the dynamic XRD (Figure 6D) it is possible to observe the peaks specific to the type II form (201) at approximately $12.7\ 2\theta$ and (002) at $20.8\ 2\theta$. It is likely that the viscous nature of the polymerized genipin reduces the mobility of the crystallizing genipin, lowering the free energy in the system and supporting the formation of the less stable form II genipin structure. On heating, the form II peaks begin to lessen in intensity after 90 °C, before disappearing completely around 97 °C. This accounts for a proportion of the melting event observed in the DSC. The remaining structure includes peaks for all the reflective planes present in form I genipin. The remaining form I crystal structure melts around 117 °C, higher than observed in the DSC experiments. This is possibly due to material inhomogeneity because of the somewhat uncontrolled nature of the polymerization reaction. It is possible that the melting form II genipin could reform into the more stable form I, giving the second melting peak. Again this would be possible because the presence of the polymer lowering the energy of this system that would support the reformation form I, when this behavior was not observable in the heating of form II in Figure 6D.

Conclusion

Two polymorphs of genipin were identified through differential scanning calorimetry and static and variable temper-

ature X-ray diffraction techniques. The more stable genipin form I has a T_m at 121 °C and a second less stable form II has a T_m at 101 °C. In both cases a structure was resolved and found to be monoclinic at room temperature. The molecular graphics demonstrate that rotation of a functional group could lead to the different packing order and stabilities. Crystals derived from dissolution in and evaporation of methanol were found to have slightly altered properties. In one sample where genipin polymerization was not evidenced, form I crystals were observed but an increase in crystal imperfection reduced the melting temperature. In another sample where polymerization did occur, the formation of the less stable form II was observed.

Acknowledgment. The author wishes to thank Unilever Research and Development Colworth, EPSRC and the Impact Faraday Partnership for the financial support of this project, and John. E. Davis at the University chemical laboratories for his assistance. We further thank the EPSRC for financial assistance towards the purchase of the Nonius CCD diffractometer.

Supporting Information Available: Crystallographic data files detailing both Reitveld refinements. This material is available free of charge via the Internet at <http://pubs.acs.org>.

References

- (1) Zhang, C.-Y.; et al. *Cell Metab.* **2006**, *3*, 417–427.
- (2) Butler, M. F.; Clark, A. H; Adams, S. *Biomacromolecules* **2006**, *7*, 2961–2970.
- (3) Khurma, J.; Rohindra, D. A. *Polym. Bull.* **2005**, *54* (3), 195–204.
- (4) Grzesiak, A. L.; et al. *J. Pharm. Sci.* **2003**, *92* (11), 2260–2271.
- (5) Otwinowski, Z.; Minor, W. *Methods Enzymol.* **1997**, *276*, 307–326.
- (6) Sheldrick, G. M. *SHELXL97 and SHELXLS97*; University of Gottingen: Germany, 1997.

CG070560A